Tectono-metamorphic and geochronological evolution of the Rengali Province in the Riamal-Rengali-Khamar sector, Odisha, India

Summary

By

ARNAB DASGUPTA
Registration No.- 14RS15110004

PRESIDENCY UNIVERSITY
KOLKATA

Supervisor:
Prof. Sankar Bose

Joint-supervisor:
Prof. Gautam Ghosh

2017

Tectono-metamorphic and geochronological evolution of the Rengali province in the Riamal-Rengali-Khamar sector, Odisha, India

(Five thousand word summary for the partial fulfilment for award of Doctor of Philosophy degree)

Arnab Dasgupta

Supervisor: Dr. Sankar Bose; Joint-supervisor: Dr. Gautam Ghosh

Introduction

Continental crust grew episodically during the Precambrian time before modern style plate tectonics was initiated. Evidences of such early Earth events are often obliterated by partial absence of rock records, multiple evidences of reworking, fragmentation and amalgamation of continents over time. Craton-margin mobile belts evolve through orogenesis with several phases of deformation and metamorphism and record the complex growth history of continents and are considered best candidate for studying continental growth history. On the eastern side of peninsular India, the Archean Singhbhum Craton (SC) and the Proterozoic Eastern Ghats Belt (EGB) occur as a craton-mobile belt couplet, which can provide insight to understand the growth history of the eastern Indian shield. The present study was carried out in the Rengali Province which occurs at the juncture of SC and EGB.

Geological background

Rengali Province (Fig. 1) is a narrow, linear WNW-ESE trending zone which is squeezed in between the SC in the north and the Proterozoic EGB in the south. The rocks of the Rengali Province are quite distinct from the Paleo-Mesoarchean medium-grade granite-greenstone sequences of SC lying in the north, as well as the Paleo-Mesoproterozoic ultrahigh temperature metamorphic rocks of the EGB. The Rengali Province is composed of a series of WNW-ESE trending tectonic zones showing contrasting lithological, metamorphic and age constraints, separated by major ductile faults or shear zones (Mahalik, 1994; Nash et al., 1996; Crowe et al., 2003; Misra and Gupta, 2014). Petrological, structural and geochronological data from this province suggest its evolution through episodic orogenic pulses since the Neoarchean time (Crowe et al., 2001, 2003; Mahapatro et al., 2012; Bose et al., 2016; Bhattacharya et al., 2016). The Rengali Province is traditionally interpreted to be dominated by strike slip faults (Dobmeier and Raith, 2003; Misra and Gupta, 2014), but proper characterization of the faults are lacking (Dobmeier and Raith, 2003). Few workers proposed an oblique collision (Bhattacharya, 1997), or lateral ramp development (Biswal et

al., 2007) was involved in the development of the Rengali Province, but detailed structural analysis integrating geometric, fabric and kinematic data with critical geochronological constraints encompassing the entire terrane is almost absent.

High precision geochronology data from Rengali Province is also scarce. Metasedimentary and metaigneous rocks from this province have 2800–2200 Ma and 3900–2900 Ma Nd-model ages (Rickers et al., 2001). High-grade granitoids from Bhuban area at the eastern part of the province yields c. 2800 Ma emplacement age ($^{207}Pb/^{206}Pb$ zircon by Misra et al., 2000); whereas Rb–Sr data from some of the charnockites yield c. 2750–2730 Ma ages (Sarkar et al., 2000). $^{40}Ar/^{39}Ar$ dating of hornblende and biotite grains from the amphibolite-grade rocks yields much younger age data of c. 700–420 Ma (Crowe et al., 2001). The latter time frame has been considered to represent a major orogenic event, yet the span of time looks unrealistically long for duration of any orogenic belt. Recently, geochronological data from the high-grade rocks from to the eastern part of the Rengali Province yield metamorphic ages of c. 3507 Ma and c. 2780 Ma (Mahapatro e al., 2012) which essentially implies late Archean orogenic events within the Rengali Province.

Objective of the study

The present work will be carried out with the following objectives:

(1) To unravel the tectonometamorphic history of the rocks of the Rengali Province from the Riamal-Rengali-Khamar sector and to explain the lithological and structural heterogeneity of the province.

(2) To build a geochronological evolutionary history of the Rengali Province and ascertain specific events of orogenesis and crustal growth. This will also help to evaluate its possible genetic linkage with the EGB or the SC.

(3) To propose a possible tectonic model for evolution of the Rengali Province.

(4) On a larger perspective, the role of the Rengali Province during the Precambrian supercontinent cycle(s) would also be attempted.

To fulfil these objectives, a small segment of the central part of the Rengali Province was selected for detailed geological investigation in this study. The Riamal-Rengali-Khamar sector surrounding the Rengali reservoir was chosen for this purpose as it provides a complete transect through the province depicting the lithological and structural heterogeneity as well as its boundary relations with the adjoining SC and EGB.

Structure and lithology

Detailed field-scale structural and microstructural analyses of the rocks from central part of Rengali Province were carried out to unravel the deformation events. These structural analyses were accompanied by radiometric dating of specific rock types to delineate the exact timing of these deformation events. Based on the field-scale structures, the province can be subdivided into several E-W and ESE-WNW trending longitudinal belts having distinct lithologies, grade of metamorphism as well as structural pattern. Regional-scale shear zones like the Riamal shear zone (RSZ) in the west and the Akul fault zone (AFZ) in the west were responsible for structural modification of these longitudinal belts. Moreover, some E-W fault splays from the RSZ also occur within the province, which actually delineate these belts. These belts are named as the Barkot shear zone (BSZ), the Northern supracrustal belt (NSB), the Central Gneissic Belt (CGB), the Southern supracrustal belt (SSB) and the Kerajang fault zone (KFZ).

The southernmost belt, the WNW-ESE striking Kerajang fault zone marks the southern boundary of the Rengali Province with the southerly placed Gondwana sedimentary basin and the EGB. This fault zone is marked by the highly sheared low-grade supracrustal rocks, mainly quartzite, mica schist and actinolite-tremolite schist that have undergone greenschist facies metamorphism. The only occurrence of calc-schist rocks is observed as an outcrop within Tikra river section. This outcrop is essentially composed of alternate bands of quartzite- mica schist -calc silicate schist. The outcrop is highly deformed and complex fold pattern is observed within it. A leucogranite (Fig. 2a), though part of the gneissic basement, is exposed within these low grade supracrustals. Foliation of the fault zone rocks varies between steeply southerly dipping to subvertical, and indicates a dextral kinematics. The fabric is essentially mylonitic in nature. A later phase of brittle deformation was identified within this zone from the presence of intensely fractured fault breccia, cataclasite and gouge zones.

SSB is consisting of quartzite and mica schist and it lies between the intensely sheared KFZ and high-grade rocks of the CGB. These rocks of the SSZ underwent up to greenschist facies metamorphism. Mean foliation within this belt is sub-vertical to steeply northerly dipping in nature. Alternate quartzite-mica schist bands display development of asymmetric fold sequences in macroscopic-scale and are characterized by steeply inclined southerly verging folds. The northern boundary between the SSB and the CGB is marked by the South Riamal Splay. Near the shear zone, the fabric is mylonitic in nature, with presence of mica fish (Fig. 2b) and S-C fabric, indicating a dextral movement. The kinematics is top-to-south reverse sense slip and can be identified by overturned asymmetric northerly verging folds.

Dominant fabric is mylonitic which is more prominent towards the fault zone. Quartzite at several locations contain ferruginous matrix which show mm to cm thick red colour bands associated with fine scale brecciation. Near the fault zone, the grade of metamorphism increases up to amphibolite facies with the development of sillimanite-fibrolite in the mica schist.

The CGB, or the centrally lying high-grade belt, can be subdivided into three parallel sub-domains, each showing distinct foliation and deformational features. The dominant lithology of this belt is represented by amphibolite-facies felsic gneiss with components of granite gneiss, garnet-biotite gneiss and migmatite hornblende gneiss. Sporadic patches of amphibolite are also present within the migmatitic hornblende gneiss. An E-W ridge of charnockite gneiss (Fig. 2c) occurs near the northern boundary of CGB and NSB, and is marked by North Riamal shear zone. Enclaves of mafic granulite (Fig. 2d) are also present within this charnockite gneiss. These charnockite gneiss and mafic granulite preserve the granulite facies mineral assemblages. This charnockite gneiss is foliated in nature and the gneissic fabric gradually changes to mylonitic near the adjacent shear zone. Intrusive pegmatite and basic sills/dykes also occur as small bodies within CGB. These intrusive units show cross-cutting relationship, but were deformed with the high-grade gneissic rocks.

Stratified supracrustal rocks showing large-scale folds crop out at the western and eastern boundary of this E-W elongated belt with the gneissic basement occupying the central part. The gneissic rocks are dominated by quartzofeldspathic and migmatitic hornblende gneiss with intrusive granitic veins, pegmatites and metabasic dykes. The gneissic rocks show amphibolite-facies assemblage of quartz-feldspar-garnet-hornblende-muscovite-biotite while the gneissic layering is demarcated by alternate melanocratic and leucocratic layers. The supracrustal sequences of the NSB are essentially comprised of BIF, metachert, metaconglomerate, metagreywacke, mica schist, chlorite-actinolite schist and quartzite. All the rocks underwent greenschist-facies metamorphism. Structural fabric points toward top-to-north shearing sense (Fig. 2f) of this belt.

To Barkot shear zone lies at the north of NSB. It can be described as a narrow zone (~500 m width) of strongly deformed rocks which include quartzite, conglomerate and pelitic rocks of the SC margin and sheared gneisses of the Rengali Province. The nearly undeformed and un-metamorphosed sandstone-conglomerate units of the SC with low and variable bedding dips change to steep southerly dip close to shear zone. The fabric is mylonitic and steep, southerly dipping foliation and a down-dip mineral lineation within the shear zone is present.

The wedge-shaped Akul fault zone (2-15 km width), developed along the eastern margin of the study area, is bounded between two NW-SE and NNW-SSE trending dextral faults. This zone is composed of low-grade volcanics and sedimentary rocks of the Malaygiri assemblage and the Tikra assemblage as well as the amphibolite-facies gneisses of the CGB and shows pervasive fold development.

Petrology

The high-grade rocks that constitute the CGB shows amphibolite- to granulite-facies mineral assemblages and these rocks are intruded by various mafic and granite bodies. Textural data of all the rocks of CGB are compared with mineral chemical data from representative samples of each rock. Petrographic study of the low-grade supracrustal rocks were also carried out.

The gneissic foliation in the charnockite gneiss is marked by alternate orthopyroxene + hornblende-rich dark band and quartzofeldspathic light bands. The rock is medium-grained and greyish in color. Dark bands contain orthopyroxene + hornblende + magnetite + ilmenite ± clinopyroxene ± biotite as well as accessory minerals like apatite and zircon in varying proportions. Granoblastic texture that typically develops in granulite facies metamorphism is conspicuous. In few samples, coronal garnet (with intergrown quartz) is present, forming on orthopyroxene and ilmenite grains (Fig. 3a). Minerals are mostly equigranular, although few porphyroblasts of perthitic feldspar are also present. Deformational features like subgrain formation and recrystallization by grain boundary migration are observed within the quartz grains. Replacement of pyroxene by hornblende in several samples suggests retrograde metamorphism that the charnockite gneiss might have suffered (Fig. 3b). Pyroxene is Fe- rich (X_{Mg} = 0.23-0.37) while hornblende is compositionally hastingsite to ferro-Tschermakite (X_{Mg}= 0.26-0.31). F and Cl contents are negligible in hornblende.

Mafic granulite enclaves contain clinopyroxene, plagioclase, garnet, quartz, magnetite, ilmenite, orthopyroxene with variable amount of hornblende and biotite. In some places, garnet-free variety of mafic granulite also occurs as enclaves. The texture of the rock is granoblastic, but gneissic fabric is well-developed in most samples. Replacement of garnet and clinopyroxene by biotite and hornblende is common (Fig. 3c). Garnet is almandine-grossular ($Alm_{60-63}Grs_{19-22}Pyp_{14-16}Sps_{3-4}$) in composition, with rimward increase of almandine and decrease of pyrope contents. Hornblende is compositionally ferropargasite, with X_{Mg} varying in the range 0.45–0.48.

Calc-silicate granofels locally occur as dismembered boudins within the charnockite gneiss. The mineral assemblage is plagioclase-garnet-quartz-epidote-sphene and accessory zircon. Garnet and epidote show intergrowth texture (Fig. 3d). Unlike garnet in other rock types, this garnet is grossular-andradite ($And_{51-57}Grs_{35-40}$) in composition. Almandine component is low (6–8 mole%) but pyrope and spessartine components are negligible (< 1 mol%). Epidote is Al-rich in nature.

Migmatitic hornblende gneiss is macroscopically similar to the charnockite gneiss, but subsequent study under microscope reveals that the rock is almost devoid of pyroxene. The mineral constituents are hornblende +K-feldspar + plagioclase + quartz +ilmenite-magnetite ± biotite ± garnet. Hornblende is Mg-poor (X_{Mg}= 0.31-0.34), and compositionally hastingsite in nature. Fe-Ti oxide is present as inclusion within hornblende porphyroblasts. The grade of metamorphism is middle-upper amphibolite facies. Evidence of deformation is present in the form of gneissic foliation in outcrop-scale, as well as from the subgrain boundary and grain boundary migration features in microscopic-scale. In some samples almandine-grossular garnet ($Alm_{68-70}Grs_{18-20}Sps_{6-7}Pyr_{5-7}$) is also present.

Granite gneiss is the most abundant rock type of the CGB. The mineral constituents are quartz, alkali feldspar and plagioclase with varying amount of biotite, muscovite, garnet, ilmenite and magnetite. Original igneous textures are mostly obliterated by metamorphism and deformation. Modal abundance of mafic mineral is usually low (< 10 modal%). The rock shows pervasive foliation by stretching of grains which locally produces a mylonitic fabric (Fig. 3e). In mylonitized granite gneiss, all the phases show extreme grain refinement. Both syn-kinematic as well as post-kinematic garnets are observed.

Amphibolite occurs as enclaves within the granite gneiss and contains coarse granoblastic aggregate of hornblende and plagioclase with variable amount of garnet and quartz. In some variety of amphibolite, garnet is absent, but clinopyroxene is present as relic (Fig. 3f). Hornblende grains are magnesian (X_{Mg} = 0.56-0.67) and compositionally calcic-amphibole (edenite to Tschermakite). Garnet in amphibolite is compositionally almandine (57-62 mole%) and grossular (20-27 mole%) in nature. Plagioclase composition is anorthite-rich (X_{An} =0.58-0.60) with insignificant orthoclase (~1 mole%) component.

Metagabbro occurs as enclave within the granite gneiss and essentially composed of plagioclase, clinopyroxene, hornblende and biotite with subordinate amount of magnetite and orthopyroxene. Original igneous textures are preserved as plagioclase and pyroxene grains show interlocking arrangement and compositional zoning plagioclase grains. Hornblende is ferropargasite in composition and shows stable grain contact with orthopyroxene and

magnetite as inclusion within orthopyroxene. Clinopyroxene is magnesian (X_{Mg} = 0.66-0.69) and slightly aluminous (Al_2O_3= 3.0-3.5 wt.%) in nature.

Metadolerite intrusives occur at several places within the CGB and show cross-cutting relationship with the basement gneisses. This rock is composed of clinopyroxene, orthopyroxene, plagioclase, Fe-Ti oxides, pyrite, amphibole and biotite. Clinopyroxene grains are more magnesian (X_{Mg} =0.64-0.70) compared to orthopyroxene (X_{Mg} = 0.45-0.48). Relic igneous features like intergranular and ophitic textures are present. Plagioclase grains are lath-shaped, calcic ($Ab_{29-41}An_{58-70}$) and shows compositional zoning. Replacement of clinopyroxene by clusters of amphibole and biotite is observed. Biotite (X_{Mg}= 0.46-0.47) contains high amount of Ti (6.3-6.9 wt.% TiO_2). All the phases show minor evidence of deformation, e.g. plagioclase laths show bending, marginal recrystallization and undulose extinction. Overall these intrusives suffer low-grade metamorphism.

The supracrustal belt and shear zones occurring as SSB and NSB are composed of low-grade quartzite, mica schist, chlorite schist. In the SSB, calc-silicate schist locally occurs within the Tikra river section. Biotite schist consists of mainly biotite which defines the schistosity. Muscovite schist is dominated by the presence of muscovite, quartz and feldspar where muscovite flakes define the schistosity. Calc-silicate schist is essentially composed of actinolite-tremolite-biotite-calcite with some amount of opaque minerals. Prominent crenulations developed within this rock type defined by actinolite-tremolite-biotite grains.

Quartzite from the southern and northern belts is mainly composed of quartz and minor amount of muscovite. Sporadic occurrence of sillimanite is present in quartzite occurring close to the major shear/fault zones. Foliation in quartzite is marked by flat quartz grains occasionally with oriented muscovite grains. Near the shear zones, this foliation changes to mylonitic. Quartzite in thin section is characterized by a mylonitic fabric where S-C structures are defined by dynamically recrystallized quartz grains. Grain size gradually decreases towards the shear zone. Near the Kerajang Fault, the greenschist facies mineral assemblage changes to amphibolite facies mineral assemblage of quartz-muscovite-sillimanite-fibrolite. Locally, muscovite shows partial breakdown to a skeletal intergrowth of K-feldspar and fibrolite which suggests an increase in temperature and the onset of incipient partial melting due to shear heating (Fig. 3h).

The leucogranite, originally part of high-grade basement of the CGB, is exposed within the schistose rocks of the SSB. This rock is composed of quartz, K-feldspar, muscovite and garnet. Garnet is post-kinematic in nature. Foliation within the sample is defined by muscovite grains.

Geothermobarometry

Conventional geothermobarometric analyses of the high-grade rocks of the CGB were done to understand the pressure and temperature conditions, under which these rocks were metamorphosed (Table 1). Peak P-T conditions for the mafic granulite were calculated from the garnet-clinopyroxene-plagioclase-quartz assemblage. The garnet-clinopyroxene (Ganguly, 1979) thermometry yields peak temperature in the range 796–846 °C and the garnet-clinopyroxene-plagioclase-quartz barometer (Moecher et al., 1988) yields pressure estimates in a range of 9.0–9.5 kbar. Textural evidences also suggest a phase of retrograde metamorphism and this is estimated using hornblende-plagioclase thermometer which yields temperatures in the range of 617-623°C at a pressure of 8 kbar. Charnockite gneiss recorded a peak metamorphic temperature the range 746–842°C at 8 kbar, deduced from the orthopyroxene-ilmenite assemblage after the model of Bishop (1980). Evidence of retrograde metamorphism is evident in charnockite gneiss and the results show similar P-T range as of the mafic granulites. Relict mineral assemblage of garnet-clinopyroxene within amphibolite yields a maximum temperature of 718°C at an assumed pressure of 8 kbar using the model of Ganguly (1979). The hornblende-plagioclase thermometer (Holland and Blundy, 1994), on the other hand, yields 578–610°C temperatures, which can be attributed to the late cooling. Metagabbro, which occurs as enclaves within the granite gneiss of CGB, yields a peak metamorphism temperature of 763°C estimated from the hornblende-plagioclase thermometer (Holland and Blundy, 1994). From the thermobarometric data, it can be inferred that mafic granulites suffered a high pressure metamorphism (~10 kbar) whereas all the other gneisses, metagabbro, amphibolite experienced amphibolite facies P-T condition followed by further cooling.

Due to resetting during post-peak cooling, the P-T conditions estimated from geo-thermobarometric calculations can produce low value. Hence, phase diagram modeling using whole rock chemical data is done. Perple_X version 6.6.8 (Connolly and Petrini, 2002) was used to estimate the P-T conditions and for modeling. A representative mafic granulite sample with a peak metamorphic assemblage Grt+Cpx+Pl+Qtz+Opx and another representative amphibolite with the peak assemblage of Hbl+Pl+Qtz+Grt+Cpx were considered for this purpose. Phase diagram calculations were done in the Na_2O-CaO-FeO-MgO-Al_2O_3-SiO_2-TiO_2-H_2O system. For the mafic granulite sample, the modal percentages of garnet and plagioclase were calculated and the values are 14–18% and 33–37% respectively. These modal values were compared with theoretically calculated isopleths and a P-T window of 10.6 ± 0.5 kbar, 860 ± 20 °C is defined to represent the peak metamorphic condition. For the amphibolite sample, modal percentages of garnet and plagioclase were

measured as 1–3% and 25–28% respectively and then compared with the theoretically calculated isopleths. It gives a peak P-T window of 8.5 ± 0.2 kbar, 800 ± 20°C.

Geochemistry

Major, trace and REE geochemistry of the high-grade rocks of CGB were done to understand the protolith history of these high-grade rocks. In charnockite gneiss, SiO_2 contents vary within a small range (66.73–71.27 wt.%). These rocks have low TiO_2 content. The major element chemistry of the migmatitic hornblende gneisses is marked by high SiO_2 (71.53–73.19 wt.%), moderate Al_2O_3, FeOt, MgO, CaO and low TiO_2. Mafic granulite is marked by intermediate SiO_2 (49–56 wt.%), high TiO_2, Al_2O_3, FeOt, MgO and CaO.

Compositions of the migmatitic hornblende gneiss, granite gneiss and the charnockite gneiss are plotted within the granite compositional field of Na_2O+K_2O vs.SiO_2 diagram. Mafic granulite and igneous intrusives are plotted within the field of gabbro and diorite. All the gneissic samples are metaluminous to very weakly peraluminous in characters with alkali-calcic to calc-alkaline trends. The charnockite gneiss shows ferroan character. REE are considered more reliable indicator for pre-metamorphic characters compared to the major or trace elements. Chondrite-normalized REE patterns for the charnockitic gneiss, migmatitic hornblende gneiss and the granite gneiss show LREE enrichment, flat HREE pattern along with a pronounced negative Eu anomaly. Tectonic discrimination plotting of trace elements suggests A-type character and within-plate tectonic setting for all the gneissic samples. From all the geochemical signatures it is inferred that the charnockite gneiss, migmatitic hornblende gneiss and the granite gneiss that constitute the CGB have evolved from the same magma.

Geochronology

A detailed zircon U–Pb geochronological analysis of the amphibolite to granulite-facies rocks and U-Pb-Th monazite chemical age dating of the supracrustal rocks from Rengali Province were carried out at the Hiroshima University, Japan (Table 2). Selective samples comprising of charnockite gneiss, migmatitic hornblende gneiss and granite gneiss were analyzed using SHRIMP and the acquired raw data were processed by the CONCH program (Nelson, 2006).

Zircon grains from the charnockite gneiss yield two statistical pools of data (95% confidence) of 2861±30 Ma and 2818±15 Ma (Fig. 5a). Spots from the high-U overgrowth yield a third pool date of 2489±23 Ma and it is probably the age of another prominent thermal overprint. Zircon grains from migmatitic hornblende gneiss show a near concordant pool age of 2828 ±9 Ma. Two spots from core region shows a slightly older age of 2860±5a Ma. A

single spot recorded a much younger age of 2471±4 Ma. It can be concluded that emplacement age of the protolith of this gneiss is around c. 2828 Ma (Fig. 5b). All the grains of mafic granulite sample show thick metamorphic overgrowth. Spot data are nearly concordant and yield a group age of 2488±19 Ma (95% confidence). An older age of 2844±7 Ma is identified from a smaller group (Fig. 5c). This older age domain of c. 2844 Ma is situated at the interior of zircon and possibly reflects a crystallization age of the protolith. The c. 2488 Ma is the most dominant tectonothermal event witnessed by this rock. Zircon grains of the felsic gneiss yield three group ages. Spots from core region yield a group age of 2776±24 Ma whereas the overgrowth domain yields a pooled age of 2508 ±14 Ma (Fig. 5d). Few other spots from the overgrowth zone of zircon yield the third age group i.e. 2434±34 Ma. However, the dominant age groups are c. 2776 Ma and 2508 Ma and it can be inferred that c. 2776 Ma is the protolith emplacement age, whereas c. 2508 Ma is the age of metamorphism. Zircon grains from the leucogranite yield a group age of 2807±13 Ma, but a single spot within an overgrowth gives an age of 2484±5 Ma (Fig. 5e). It can be inferred that possibly this leucogranite was emplaced at c. 2807 Ma and a later metamorphism affected it at c. 2484 Ma.

Chemical age dating of monazite from shear zone samples was also carried out. The leucogranite sample contains monazite showing uniform single population age of 498 ±4Ma and probability density plot shows a strong peak at c. 500 Ma (Fig. 5f). Another sample of highly foliated medium-grade rock of SSB with mineral assemblage quartz-K-feldspar-muscovite-sillimanite-magnetite was also analyzed for monazite. Analyzed spots show dates between c. 507-554 Ma. Statistical analyses yield two peak population of 521±3 Ma and 542±5 Ma.

Discussion

Detailed structural mapping and microstructure analysis reveals that Rengali Province is composed of several litho units of contrasting deformational pattern, as well as metamorphic grade and is separated by several regional-scale shear zones. The structural style can be inferred as strike slip faulting coupled with N-S shortening and development of fold-thrust belt. The EGB-Rengali Province boundary can be classified as transpression or oblique-slip boundary. In the present study, field observations on cross cutting relationships among different structural systems indicate absence of clear superposition order which suggest that these systems developed at a similar time or at least were active during the same tectonic event. The five shear or fault zones have been separated based on minor variation in foliation, lineation, fold, fabric. Transpressional deformation in all zones was strongly partitioned over

the study area. Overall, the strike slip component is concentrated in narrow shear zones or discrete faults; the KFZ, the RSZ and the AFZ are the examples of such strike slip zones with small variations in structural details. These zones are principally characterized by sub-vertical foliation, predominantly sub-horizontal lineation and asymmetric Z-folds on surface associated with a strong dextral strike slip deformation. On the other hand, except the narrow BSZ at the northern margin, shortening dominant deformation is prevalent over wider zones, displaying sub-vertical to steeply dipping S-L tectonites that grades to mylonites along zonal boundaries. Here reverse dip-slip kinematics is predominant in sub-vertical planes which indicate presence of major thrusts. The SSB, NSB and subdomains in CGB are examples of such shortening dominant zones. Transpressional fault system of Rengali Province is modified by presence of antithetic and fault systems. Accordingly, KFZ and BSZ are the main bounding faults parallel to the transpression zone boundary, while the AFZ and the RSZ are the synthetic and antithetic fault systems respectively. This resulted in the regional-scale positive flower structure, characterized by oppositely verging supracrustal-gneiss slices originating from a steep central root zone and bounded between two sub-parallel fault systems. Such thrusting of the mid-crustal gneissic basement over the upper crustal low-grade supracrustal also resulted in sharp change in metamorphic grade across the North Riamal Splay and the South Riamal Splay marking the supracrustal-CGB contact, suggesting a vertical extrusion and thrust loading from transpression.

Mineral assemblages, textures, thermobarometric results and phase diagram modelling of different lithounits of the CGB are combined to identify the important tectonothermal imprints. Charnockite gneiss and the mafic granulite preserve granulite facies metamorphic assemblages which signify lower crustal condition. Mafic granulite shows textures of subsolidus cooling (exsolved magnetite blebs) that indicate a magmatic origin of this rock. There is no clear evidence of the nature of emplacement of the protolith (mafic magma) within the deep crust, but zircon U-Pb SHRIMP data of one sample indicate a possible emplacement age of 2844±7 Ma. On the other hand, U-Pb zircon data from the charnockite gneiss suggest a possible emplacement age of the protolith as 2861±30 Ma. U-Pb radiometric dating of migmatitic hornblende gneiss, granite gneiss and the leucogranite suggest their protolith emplacement ages of 2828 ± 9 Ma, 2807 ± 13 Ma and 2776 ± 24 Ma respectively. Zircon overgrowth and partial recrystallization in the charnockite gneiss occurred at 2818 ± 15 Ma which is interpreted as the timing of high-grade metamorphism, whose peak P-T conditions are recorded in the mafic granulites of CGB. All the rocks of the CGB witnessed a second phase of high-grade metamorphism at c. 2500 Ma, but its exact textural signatures are not prominent.

The origin of the granitoid suite of the CGB can be attributed to the process of fractionation during magmatic crystallization. Interplating or underplating of basaltic magma could act as a heat source, which may lead to partial melting, assimilation of lower crustal granulite and finally fractionation of the silicic melt. The evolved counterpart of the suite, i.e. the charnockite-granite association could be explained by the duality of fluid regime. Accordingly, charnockite crystallized from magma enriched in CO_2-rich fluid while the hornblende and biotite-bearing granites could be produced from more hydrous fluid (H_2O)-dominated residual melt during the course of evolution in the same source magma. The deep seated magma would dissolve more CO_2 which will be released at shallower level by exsolution during ascent. A-type granite characteristics can be acquired in variable tectonic settings including extensional setting and accretional arc setting. In this case, it may be possible that emplacement of charnockite took place as in a syn-collisional setting followed by post-collisional emplacement of granite.

The supercontinental cycle hypothesis indicates that the earliest fragments of the protocontinents were amalgamated in the form of "Ur" (Rogers and Santosh, 2003). It was argued that the major crust binding activities in the "Ur" occurred during 3.0-2.7 Ga. This was followed by the last tectonothermal event at c. 2.5 Ga when other continental fragments became part of the "expanded Ur" (Rogers and Santosh, 2003). The present petrological, structural, geochemical and geochronological data imply that the CGB component of the Rengali Province can be considered as a part of "Ur", which has already been proposed earlier (Mahapatro et al., 2012). The c. 3.0-2.5 Ga events in the Rengali Province can also be viewed as the growth process of the SC along its southern margin. Although the Rengali Province is located adjacent to the Proterozoic EGB, the imprints of c. 1000–900 Ma strong granulite-facies metamorphism of the later terrane is rarely preserved in the Rengali Province, whereas the sheared rock at the southern boundary of Rengali Province records a thermal imprint at c. 500 Ma., which suggests a reactivation of the existing fault system during Pan-African event (c. 500-530 Ma).

Conclusion

Rengali Province is characterized by varying rock types showing widely contrasting metamorphic, structural and geochronological features. These rock units are separated by a number of WNW trending tectonic zones. Petrological, structural and geochronological data from this province suggest its evolution through episodic orogenic pulses since the Neoarchean time (Fig. 6). Though major part of the province was stabilized at c. 3000 Ma, its components continued to grow through repeated tectonothermal processes until c. 2500 Ma.

In this context, it can be defined that Rengali Province may have a share of the Neoarchean history of the supercontinent "Ur". The strong c. 1000-900 ma tectonothermal events of the southerly placed EGB is seldom present in the gneissic rocks of the Rengali Province, but Pan-African (c. 550-500 Ma) shearing eventually juxtaposed all the blocks in the present day configuration (Fig. 6).

References

Anderson, J.L., Smith, D.R., 1995. The effects of temperature and fO_2 on the Al-in-hornblende barometer. American Mineralogist 80, 549-559.

Bhattacharya, A., Das, H., Bell, E., Bhattacharya, A., Chatterjee, N., Dutt, A., Saha, L., 2016. Restoration of Late Neoarchean–early cambrian tectonics in the Rengali orogen and its environs (eastern India): The Antarctic connection. Lithos 263, 190-212.

Bhattacharya, S., 1997. Evolution of Eastern Ghats granulite belt of India in a compressional tectonic regime and juxtaposition against Iron Ore Craton of Singhbhum by oblique collision-transpression. Journal of Earth System Science 106, 65-75.

Bishop, F., 1980. The distribution of Fe^{2+} and Mg between coexisting ilmenite and pyroxene with applications to geothermometry. American Journal of Science 280, 46-77.

Biswal, T.K., De Waele, B., Ahuja, H., 2007. Timing and dynamics of the juxtaposition of the Eastern Ghats Mobile Belt against the Bhandara Craton, India: a structural and zircon U-Pb SHRIMP study of the fold-thrust belt and associated nepheline syenite plutons. Tectonics 26.

Bose, S., Das, K., Kimura, K., Hidaka, H., Dasgupta, A., Ghosh, G., Mukhopadhyay, J., 2016. Neoarchean tectonothermal imprints in the Rengali Province, eastern India and their implication on the growth of Singhbhum Craton: Evidence from zircon U-Pb SHRIMP data. Journal of Metamorphic Geology 34, 743-764.

Connolly, J., Petrini, K., 2002. An automated strategy for calculation of phase diagram sections and retrieval of rock properties as a function of physical conditions. Journal of Metamorphic Geology 20, 697-708.

Crowe, W.A., Cosca, M.A., Harris, L.B., 2001. $^{40}Ar/^{39}Ar$ geochronolgy and Neoproterozoic tectonics along the northern margin of the Eastern Ghats Belt in north Orissa, India. Precambrian Research 108, 237-266.

Crowe, W.A., Nash, C.R., Harris, L.B., Leeming, P.M., Rankin, L.R., 2003. The geology of the Rengali Province: implications for the tectonic development of northern Orissa, India. Journal of Asian Earth Sciences 21, 697-710.

Dasgupta, S., Sengupta, P., Guha, D., Fukuoka, M., 1991. A refined garnet-biotite Fe− Mg exchange geothermometer and its application in amphibolites and granulites. Contributions to Mineralogy and Petrology 109, 130-137.

Dobmeier, C.J., Raith, M.M., 2003. Crustal architecture and evolution of the Eastern Ghats Belt and adjacent regions of India. Geological Society, London, Special Publications 206, 145-168.

Eby, G.N., 1992. Chemical subdivision of the A-type granitoids: petrogenetic and tectonic implications. Geology 20, 641-644.

Ganguly, J., 1979. Garnet and clinopyroxene solid solutions, and geothermometry based on Fe-Mg distribution coefficient. Geochimica et Cosmochimica Acta 43, 1021-1029.

Holland, T., Blundy, J., 1994. Non-ideal interactions in calcic amphiboles and their bearing on amphibole-plagioclase thermometry. Contributions to Mineralogy and Petrology 116, 433-447.

Kar, R., Bhattacharya, S., Sheraton, J., 2003. Hornblende-dehydration melting in mafic rocks and the link between massif-type charnockite and associated granulites, Eastern Ghats Granulite Belt, India. Contributions to Mineralogy and Petrology 145, 707-729.

Kretz, R., 1982. Transfer and exchange equilibria in a portion of the pyroxene quadrilateral as deduced from natural and experimental data. Geochimica et Cosmochimica Acta 46, 411-421.

Mahalik, N., 1994. Geology of the contact between the Eastern Ghats belt and North Orissa craton, India. Geological Society of India 44, 41-51.

Mahapatro, S., Pant, N., Bhowmik, S., Tripathy, A., Nanda, J., 2012. Archaean granulite facies metamorphism at the Singhbhum Craton–Eastern Ghats Mobile Belt interface: implication for the Ur supercontinent assembly. Geological Journal 47, 312-333.

McCarthy, T.A., Patino Douce., A.E., 1998. Empirical calibration of the silica–Ca-tschermak's–anorthite (SCAn) geobarometer. Journal of Metamorphic Geology 16, 675-686.

Misra, S., Gupta, S., 2014. Superposed deformation and inherited structures in an ancient dilational step-over zone: Post-mortem of the Rengali Province, India. Journal of Structural Geology 59, 1-17.

Misra, S., Moitra, S., Bhattacharya, S., Sivaraman, T., 2000. Archean Granitoids at the Contact of Eastern Ghat Granulite Belt and Singhbhum-Orissa Craton, in Bhuban-Rengali Sector, Orissa, India. Gondwana Research 3, 205-213.

Moecher, D., Essene, E., Anovitz, L.M., 1988. Calculation and application of clinopyroxene-garnet-plagioclase-quartz geobarometers. Contributions to Mineralogy and Petrology 100, 92-106.

Nash, C., Rankin, L., Leeming, P., Harris, L., 1996. Delineation of lithostructural domains in northern Orissa (India) from Landsat Thematic Mapper imagery. Tectonophysics 260, 245-257.

Nelson, D.R., 2006. CONCH: A Visual Basic program for interactive processing of ion-microprobe analytical data. Computers & Geosciences 32, 1479-1498.

Nelson, D.R., Bhattacharya, H., Thern, E.R., Altermann, W., 2014. Geochemical and ion-microprobe U–Pb zircon constraints on the Archaean evolution of Singhbhum Craton, eastern India. Precambrian Research 255, 412-432.

Pearce, J.A., Harris, N.B., Tindle, A.G., 1984. Trace element discrimination diagrams for the tectonic interpretation of granitic rocks. Journal of Petrology 25, 956-983.

Pownceby, M.I., Wall, V.J., O'Neill, H.S.C., 1987. Fe-Mn partitioning between garnet and ilmenite: experimental calibration and applications. Contributions to Mineralogy and Petrology 97, 116-126.

Rickers, K., Mezger, K., Raith, M.M., 2001. Evolution of the continental crust in the Proterozoic Eastern Ghats Belt, India and new constraints for Rodinia reconstruction: implications from Sm–Nd, Rb–Sr and Pb–Pb isotopes. Precambrian Research 112, 183-210.

Rogers, J.J., Santosh, M., 2003. Supercontinents in Earth history. Gondwana Research, 6, 357-368.

Sarkar, A., Pati, U., Panda, P., Patra, P., Kundu, H., Ghosh, S., 2000. Late-Archaean charnockitic rocks from the northern marginal zones of the Eastern Ghats Belt: A geochronological study. Geol. Surv. India Spec. Pub. 57, 171-179.

1)

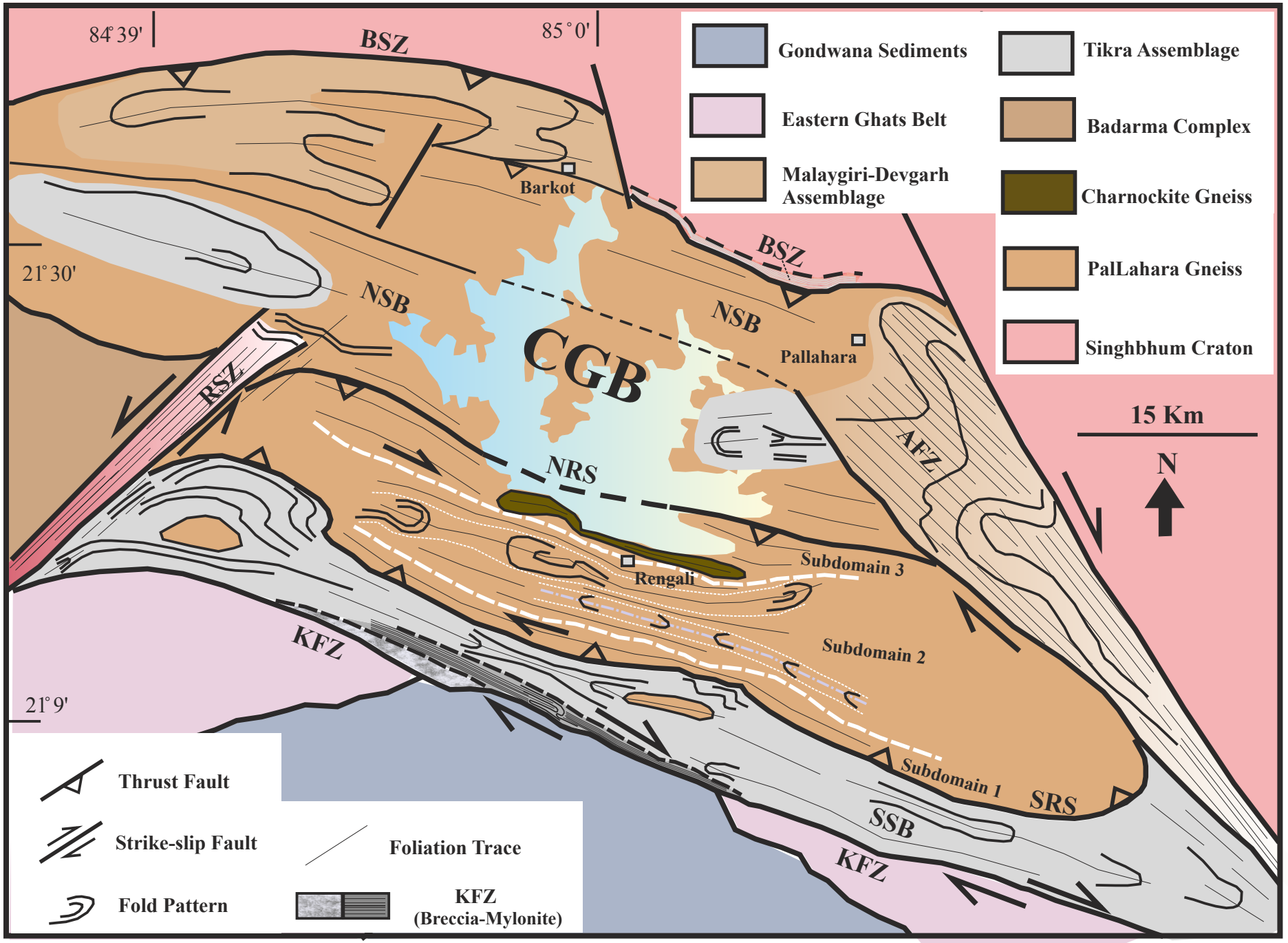

Fig. 1 Geological map of the study area of the Rengali Province, showing the main lithological units as well as the structural features (modified after *Ghosh et al., 2016*).

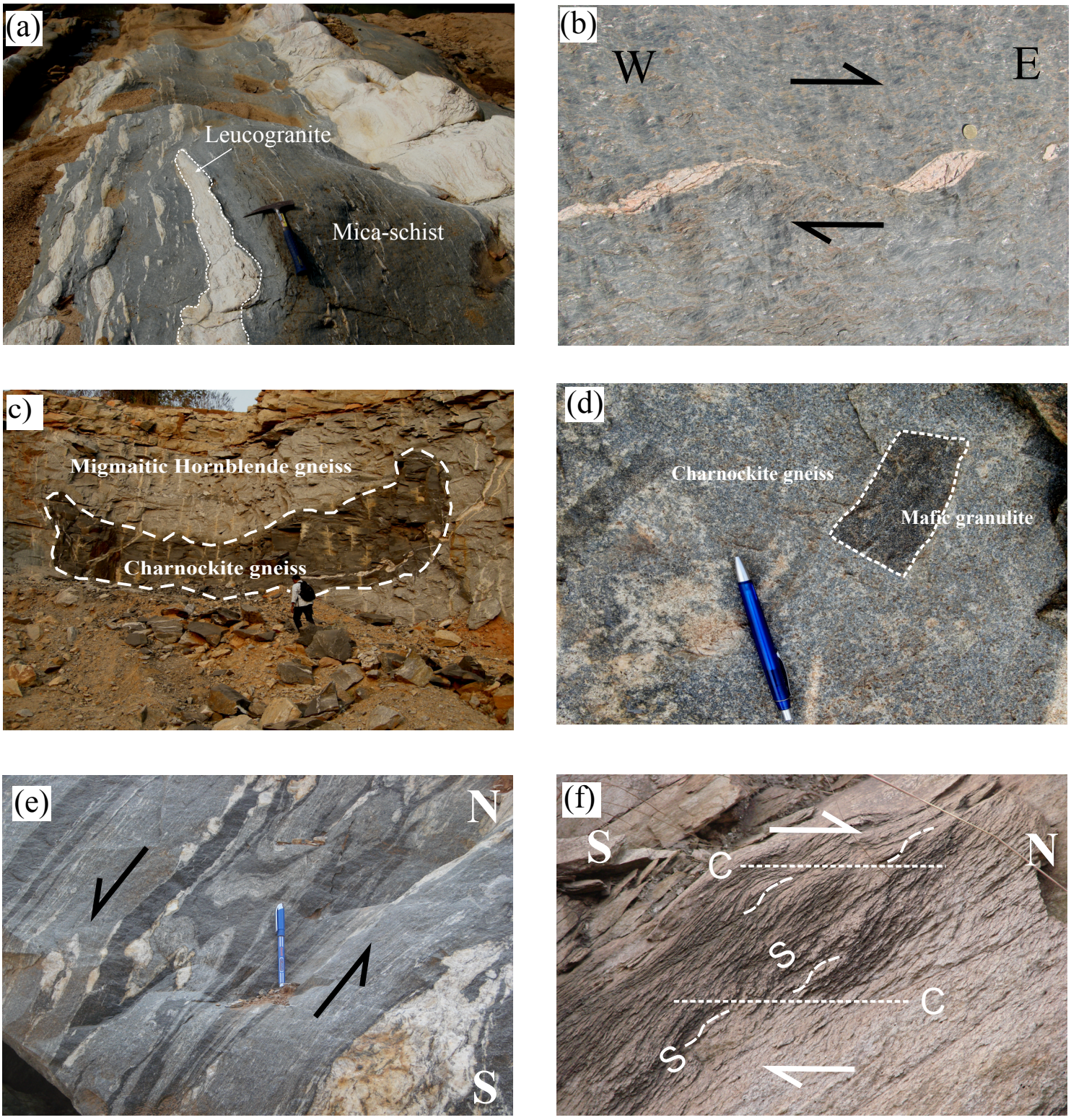

Fig. 2 Field photographs of high grade rocks and low grade supracrustals from Rengali Province. (a) Leucogranite; part of Central Gneissic Belt, exposed within low grade schistose rocks of Southern Supracrustal Belt. (b) Plan view of asymmetric 'fish' structures developed in boudinaged leucogranite layers within biotite schist. (c) Charnockite gneiss enclave within the migmatitic hornblende gneiss. (d) Mafic granulite enclave within charnockite gneiss. (e) Asymmteric northerly verging folds developed in charnockite gneiss, section view. (f) S-C fabric developed in quartzite mylonite indicating top-tothe-north slip sense.

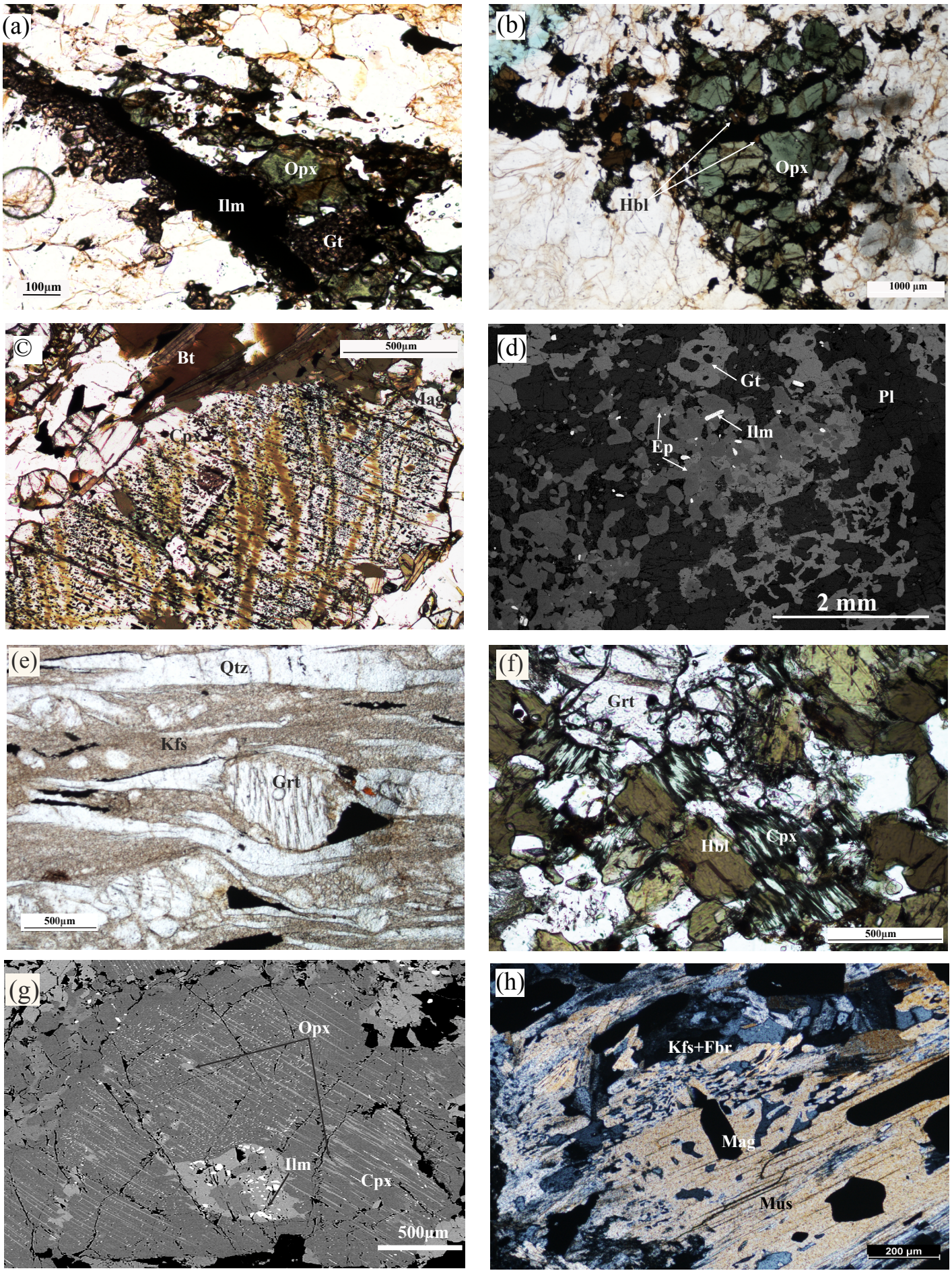

Fig. 3 Photomicrograph and BSE image of representative samples from Rengali Province. (a) Development of coronal garnet intergrown with quartz (Grt +Qtz) around orthopyroxene (Opx) and ilmenite (Ilm) against plagioclase (Pl) in charnockite gneiss. (b) Hornblende (Hbl) along the boundaries of porphyroblastic orthopyroxene (Opx) in the charnockite gneiss. (c) Exsolved magnetite (Mag) blebs within clinopyroxene (Cpx) grains in mafic granulite. (d) Interlocking texture of garnet and epidote in calc-silicate granofels. (e) Mylonitized granite gneiss showing quartz (Qtz) ribbons and deformed K-feldspar (Kfs) porphyroclasts. (f) Relict clinopyroxene in amphibolite (g) exsolved lamellae of orthopyroxene within clinopyroxene in metagabbro, with tiny needles of ilmenite (Ilm) within exsolved orthopyroxene in metagabbro (h) Muscovite flakes show breakdown to skeletal intergrowth K-feldspar and fibrous sillimanite in muscovite schist.

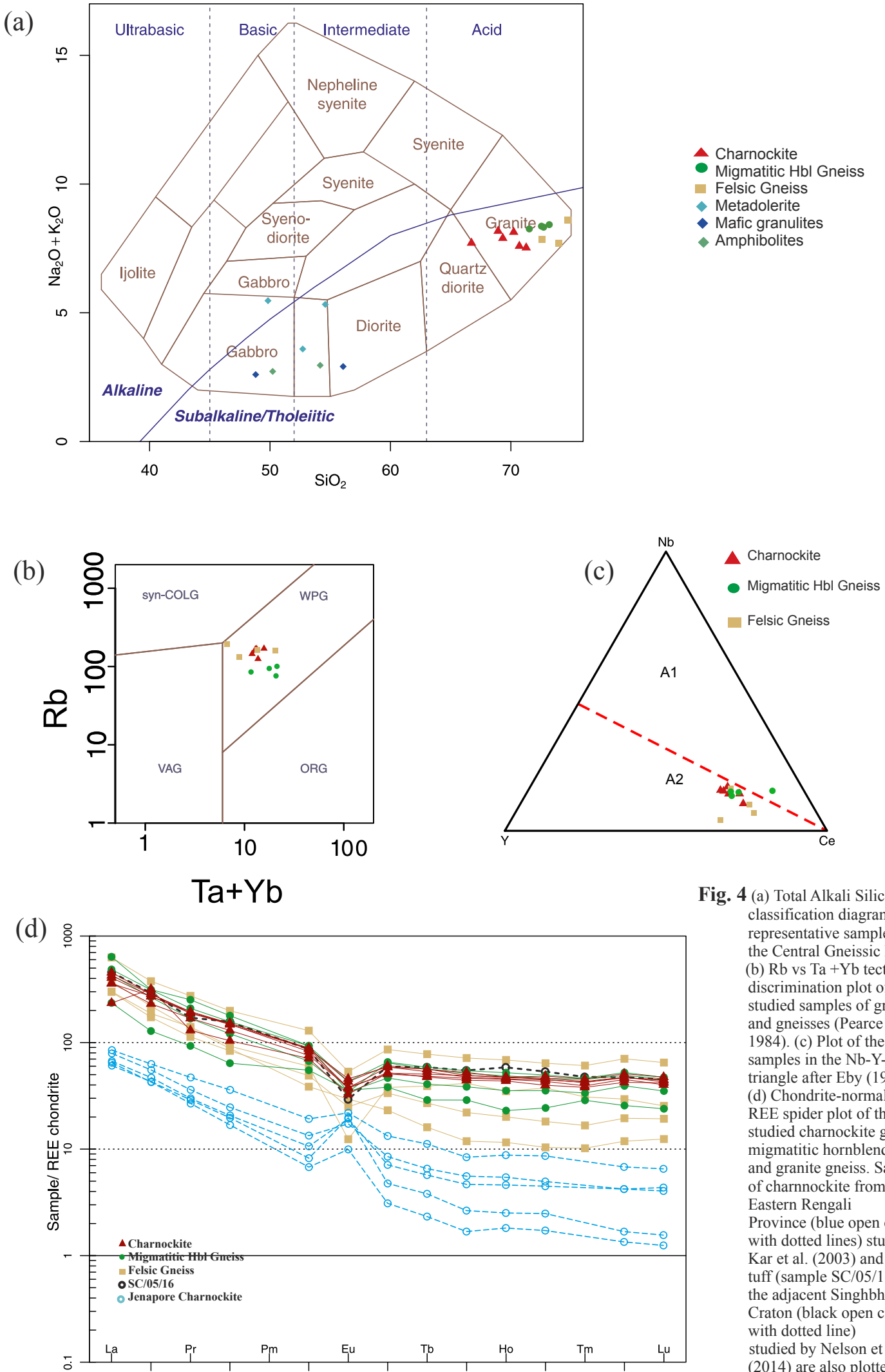

Fig. 4 (a) Total Alkali Silica (TAS) classification diagram of representative samples from the Central Gneissic Belt. (b) Rb vs Ta +Yb tectonic discrimination plot of the studied samples of granitoids and gneisses (Pearce et al., 1984). (c) Plot of the studied samples in the Nb-Y-Ce triangle after Eby (1992). (d) Chondrite-normalized REE spider plot of the studied charnockite gneiss, migmatitic hornblende gneiss and granite gneiss. Samples of charnnockite from the Eastern Rengali Province (blue open circles with dotted lines) studied by Kar et al. (2003) and dacitic tuff (sample SC/05/16) from the adjacent Singhbhum Craton (black open circles with dotted line) studied by Nelson et al. (2014) are also plotted for comparison.

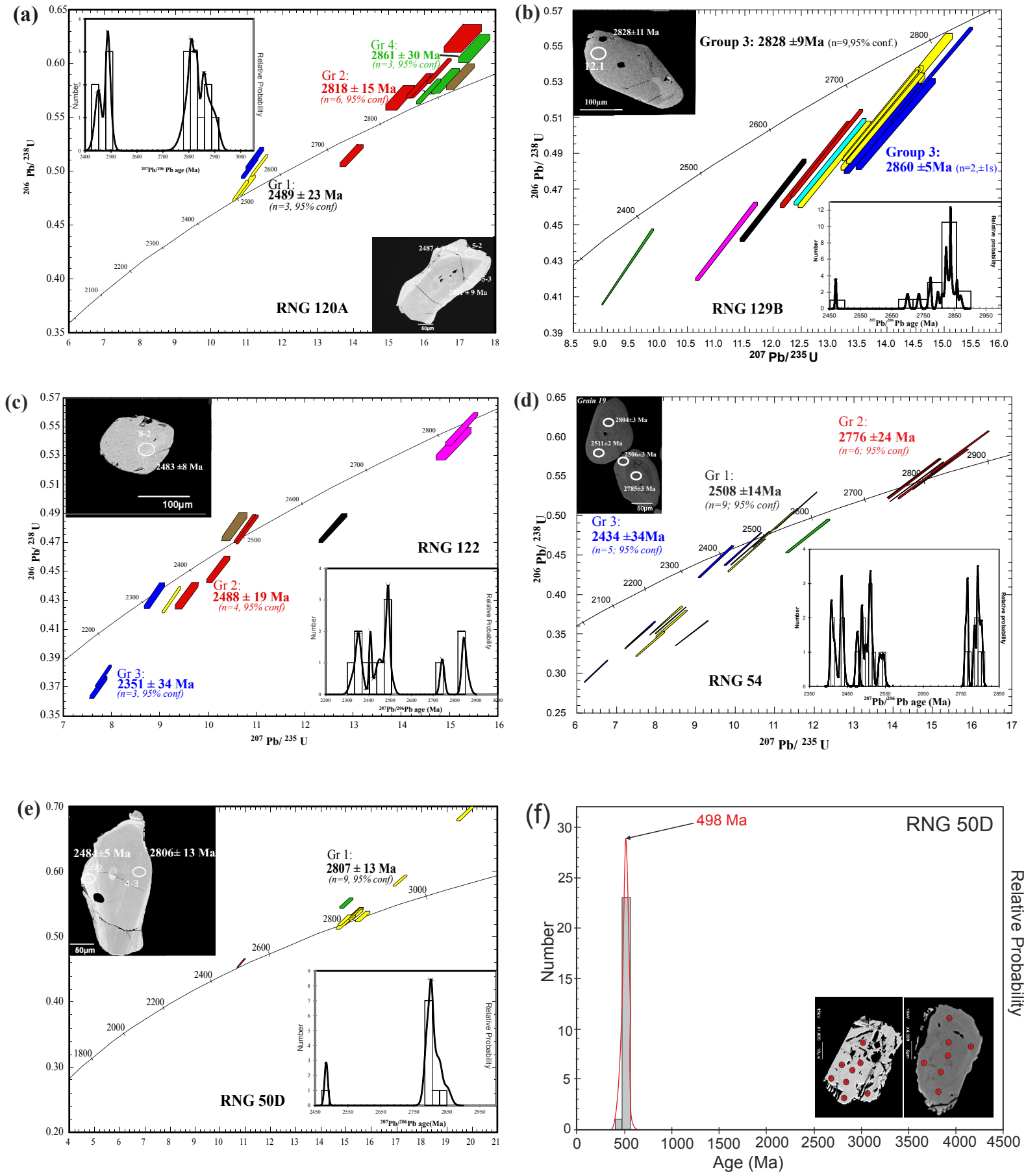

Fig. 5 Zircon (a-e) and monazite (f) ages of selected samples of the Central Gneissic Complex of the Rengali Province. Backscatter Electron Images of representative zircon grains with analyzed spots are shown in inset of each sample. (a) Charnockite gneiss sample RNG 120A; (b) Migmatitic hornblende gneiss sample RNG 129B (c) Mafic granlite sample RNG 122; (d) Felsic gneiss sample RNG 54; (e) Leucogranite sample RNG 50D; (f) Probability density plot of monazite analyzed from the leucogranite sample RNG 50D.

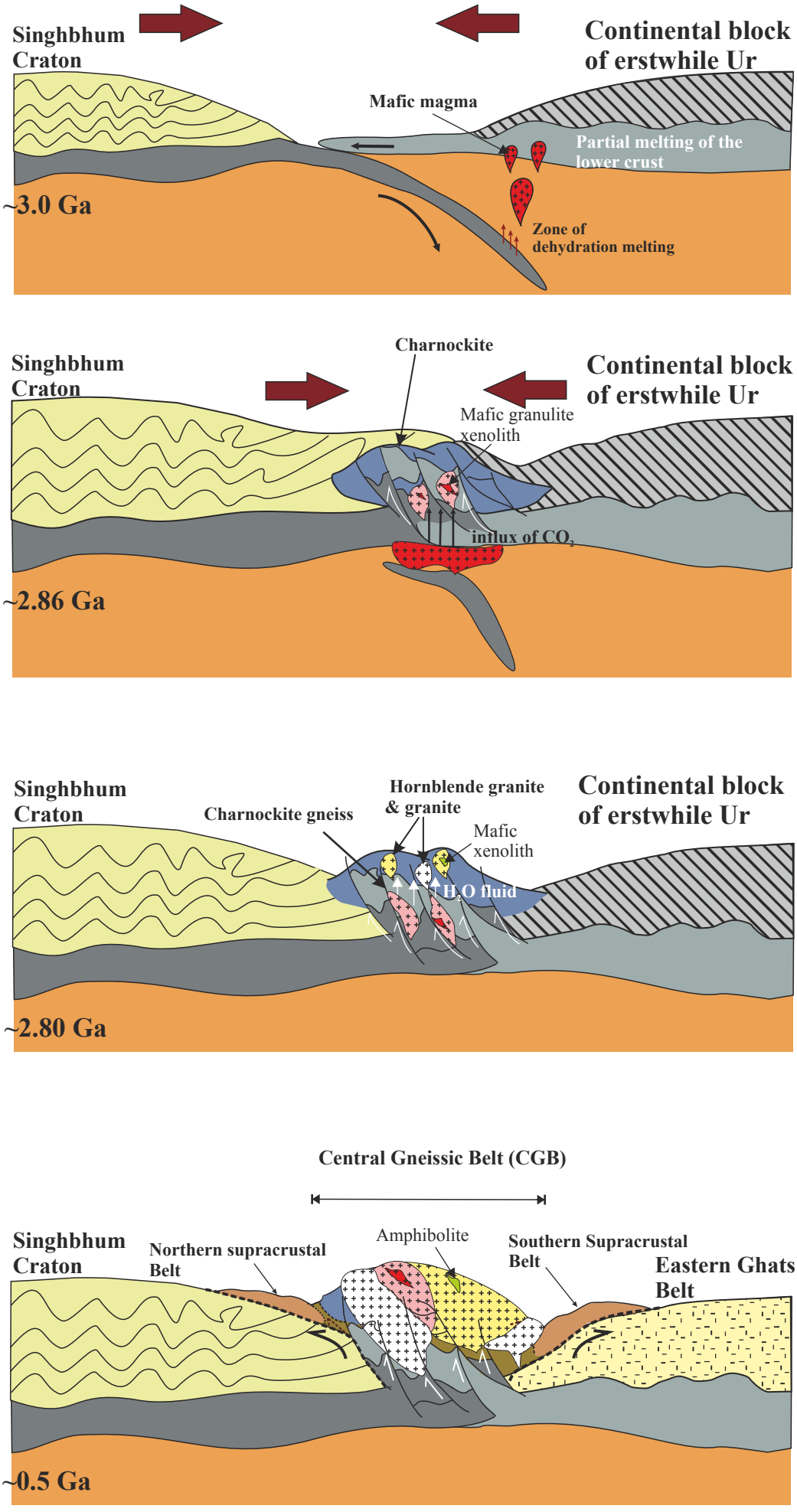

Fig. 6 Schematic diagram representing the tectonic evolution of the Central part of Rengali Province based on the available structural, petrological and geochronological data.

Table 1: Summary of pressure-temperature estimates from the studied high grade rocks of the Central Gneissic Belt.

Sample No.	Rock type	Thermo/barometer used	Model	Assumed P/T	Result
RNG 122	Mafic Granulite	Grt-Cpx thermometer	Ganguly (1979)	10 kbar	749-782°C
		GCPQ (Di- barometer)	Moecher et al. (1988)	782°C	9.5 kbar
		GCPQ (Hd- barometer)	Moecher et al. (1988)	782°C	13.2 kbar
		Al -in -Hbl barometer	Anderson and Smith (1995)	600°C	7.44 kbar
RNG 132B	Mafic Granulite	Grt-Cpx thermometer	Ganguly (1979)	10 kbar	796.5-845.7°C
		Grt-Bt thermometer	Dasgupta et al. (1991)	6.5 kbar	700-735.9°C
		Hbl-Pl thermometer	Holland and Blundy (1994)	8 kbar	617-623°C
		Silica-CaTs-Anorthite barometer	McCarthy and Patino Douce (1998)	846°C	10.91 kbar
		GCPQ (Di- barometer)	Moecher et al. (1988)	846°C	9.0 kbar
		GCPQ (Hd- barometer)	Moecher et al. (1988)	846°C	12.8 kbar
		Al -in -Hbl barometer	Anderson and Smith (1995)	620°C	7.54 kbar
RNG 146C	Hornblende Gneiss	Hbl-Pl thermometer	Holland and Blundy (1994)	8.0 kbar	696°C
		Hbl-Pl barometry	Anderson and Smith (1995)		6.19 kbar & 684.9°C
		Al -in -Hbl barometer	Anderson and Smith (1995)	690°C	5.93 kbar
RNG 102C	Hornblende Gneiss	Grt-Bt thermometry	Dasgupta et al. (1991)	6.5 kbar	594-695°C
		Grt-Ilm thermometry	Pownceby et al. (1987)		594-673°C
		Al -in -Hbl barometer	Anderson and Smith (1995)	695°C	6.20 kbar
RNG 120A	Charnockite	Opx-Ilm thermometer	Bishop et al. (1980)	8.0 kbar	712-822.5°C
		Hbl-Pl thermometry	Holland and Blundy (1994)	8.0 kbar	677.3°C
		Al -in -Hbl barometer	Anderson and Smith (1995)	677°C	6.07 kbar
RNG 158	Charnockite	Silica-CaTs-Anorthite barometer	McCarthy and Patino Douce (1998)	842°C	7.20 kbar
		Al -in -Hbl barometer	Anderson and Smith (1995)	700°C	6.26 kbar
RNG 283	Amphibolite	Hbl-Pl thermometry	Holland and Blundy (1994)	8.0 kbar	578-610°C
		Al -in -Hbl barometer	Anderson and Smith (1995)	600°C	7.01 kbar
		Grt-Cpx thermometer	Ganguly (1979)	8.0 kbar	717.91°C
		GCPQ (Di- barometer)	Moecher et al. (1988)	600°C	6.5 kbar
		Hbl-Pl thermometer	Holland and Blundy (1994)	8.0 kbar	763.8°C
			Anderson and Smith (1995)	755°C	7.43 kbar
RNG 214	Metagabbro	Two pyroxene thermometer	Kretz (1992)		653-664°C
		Al -in -Hbl barometer	Anderson and Smith (1995)	763°C	6.89 kbar

Table 2: Geochronological summary of the representaive samples fromthis study

Rock Type	Sample No.	Location	Mineral Assemblage	Rock Association	Analytical technique used	Age Data
Charnockite	RNG 120A	21°16'31.70"N 85°1'49.89"E	Qtz-Kfs-Pl-Opx-Hbl-Zrn	Exposed within a linear belt in strike continuity of the hornblende gneiss	**U-Pb SHRIMP dating of zircon**	2861 ± 30 Ma - Magmatic emplacement age 2818 ± 15 Ma - Metamorphic age 2489 ± 23 Ma - Spot date, possible metamorphic
Mafic granulite	RNG 122	21°15'33.32"N 85°4'4.83"E	Grt-Cpx-Pl-Qtz-Hbl-Opx-Ilm-Zrn	Exposed as a small enclave within charnockitic gneiss		2844 ± 7 Ma - Magmatic or metamorphic age 2488 ± 19 Ma - Metamorphic age
Migmatitic hornblende gneiss	RNG 129B	21°15'14.34"N 85°1'6.6"E	Hbl-Pl-Qtz-Kfs-Ap-Ilm-Zrn	Tonalitic rock emplaced at mid-crustal conditions. Hbl–Pl–Qtz assemblage suggests mid-crustal metamorphism		2860 ± 5 Ma - Inherited (core) age 2828 ± 9 Ma - Magmatic emplacement age 2471 ± 4 Ma - Spot date, possible metamorphic age
Felsic gneiss	RNG 54	21°16'9.72"N 85°2'15.18"E	Pl-Qtz-Kfs-Ilm-Zrn	Granite emplaced at mid-crustal level and subsequently deformed and metamorphosed at amphibolite grade.		2776 ± 24 Ma - Magmatic emplacement age 2508 ± 14 Ma - Metamorphic age
Leucogranite	RNG 50D	21°12'1.12"N 84°52'49.31"E	Qtz-Kfs-Pl-Grt-Mus-Zrn-Mnz	Exposed as a part of the gneissic basement within greenschist-grade supracrustal rocks		2807 ± 13 Ma - Magmatic emplacement age 2484 ± 5 Ma - Spot date, possible metamorphic age
Leucogranite	RNG 50D	21°12'1.12"N 84°52'49.31"E	Qtz-Kfs-Pl-Grt-Mus-Zrn-Mnz	Exposed as a part of the gneissic basement within greenschist-grade supracrustal rocks	**U-Pb-Th chemical age dating of monazite**	498 ± 4 Ma
Muscovite-fibrolite schist	RNG 209	21°14'19.42"N 84°53'3.35"E	Qrtz-Kfs-Mus-Sil-Fbr-Mag	Highly foliated schistose rock, adjacent to shear zone, showing amphibolite grade assemblage		521±3 Ma ; 542±5 Ma